**Part of Topical Section on
Emerging Semiconducting Oxides**

physica **pss** status solidi a

www.pss-a.com

applications and materials science

Temperature-dependent electrical characterization of exfoliated β-Ga$_2$O$_3$ micro flakes

R. Mitdank[1], S. Dusari[1], C. Bülow[1], M. Albrecht[2], Z. Galazka[2], and S. F. Fischer*,[1]

[1] AG Neue Materialien, Humboldt-Universität zu Berlin, 10099 Berlin, Germany
[2] Leibniz Institute for Crystal Growth, Max-Born-Straße 2, 12489 Berlin, Germany

* Corresponding author: e-mail **sfischer@physik.hu-berlin.de**, Phone: +49 30 20938044, Fax: +49 30 20937760

Among the transparent semiconducting oxides β-Ga$_2$O$_3$ is of high interest because of its wide-band gap of 4.8 eV and the corresponding transparency from deep ultraviolet to near infrared spectra. Here, we report on the preparation, structural and temperature-dependent electrical characterization of thin β-Ga$_2$O$_3$ micro flakes. β-Ga$_2$O$_3$ single crystals are grown using Czochralski technique. Micro flakes are prepared via exfoliation technique in the thickness range from 2.4 to 300 nm. The samples are characterized using confocal microscopy, atomic force microscopy, scanning electron microscopy and transmission electron microscopy. Transport investigations of β-Ga$_2$O$_3$ micro flakes are performed in the temperature range from 30 to 300 K. The electrical parameters of flakes with thicknesses larger than 100 nm correspond to those of the source bulk single crystals of highest purity and mobility. The electrical resistivity at room temperature amounts to $\rho(293\,\text{K}) = (1.5 \pm 0.5)\,\Omega\,\text{cm}$. The temperature-dependent resistivity has a minimum at $T = 130\,\text{K}$ of about $\rho(130\,\text{K}) \sim 1\,\Omega\,\text{cm}$. This finds an explanation in the maximum of the bulk mobility. From the increase of $\rho(T)$ between 130 and 300 K we determine an activation energy of $E_a = (-10.5 \pm 0.4)\,\text{meV}$. For temperatures below 50 K $\rho(T)$ increases indicating a freeze-out of charge carriers. The non-alloyed Ti/β-Ga$_2$O$_3$ metal-semiconductor contact resistance grows inverse with temperature as expected for thermionic emission. At room temperature the Ti/β-Ga$_2$O$_3$ contact resistance is comparable to the resistance of the flake for low current densities of $j < 100\,\text{A}\,\text{cm}^{-2}$. However, at high current densities $j > 100\,\text{A}\,\text{cm}^{-2}$ this contact resistance is negligible.

1 Introduction β-Ga$_2$O$_3$ is emerging as a material of interest for a variety of electronic applications. This semiconductor has gained substantial interest in the community in part because of its wide band gap (4.8 eV at room temperature [1, 2]). Advantages connected with the large band gap consist of high breakdown voltages, ability to sustain large electric fields, lower noise generation and high-power and high operating temperatures [3, 4]. A large band gap combined with its transparency and semiconductivity makes β-Ga$_2$O$_3$ a potential material for a diversity of applications. It is used in various areas like opto-electronics in the deep ultra violet range [5], thin-film electrolumines-cent displays [6], transparent field-effect transistors [4, 7] and as high temperature gas sensors [8].

In addition to the bulk properties, low dimensional β-Ga$_2$O$_3$ has received recently considerable attention due to their distinctive opto-electronic and electronic properties.

There are several studies on synthesis and characterization of β-Ga$_2$O$_3$ thin films [9], nanowires [10], nano sheets and nanobelts [11]. Polycrystalline thin films or expitaxial layers of lower crystalline quality than the bulk single crystals of β-Ga$_2$O$_3$ have been grown by different techniques like pulsed laser deposition [12], plasma-assisted molecular beam epitaxy [13], and RF magnetron sputtering [14]. However, a number of fundamental questions like origin of shallow/deep donor levels (oxygen vacancies and residual impurities including hydrogen) and corresponding electronic transport is still under debate [15–17]. Resolving these issues will require epitaxial films that can be grown under a maximum of control in crystal structure, minimum of defects and full control of the doping concentration and dopants. However, by epitaxial growth methods only α and γ-Ga$_2$O$_3$ are successfully grown, but for the β-Ga$_2$O$_3$ phase the growth of high quality epitaxial films is a matter of severe

issues and not easily achieved [9, 18, 19]. Therefore thin single crystalline films of high purity are not widely available at present.
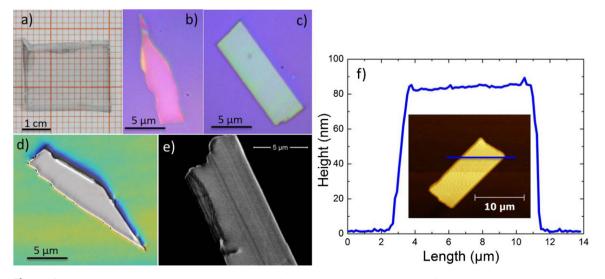
In order to pursue research on transport phenomena in single crystalline thin β-Ga$_2$O$_3$-films despite these growth issues we follow a different route for the fabrication of thin films. Such a route is given by the research on two-dimensional materials (2D) beyond graphene in which layered systems can manifest physical properties that are very different from those of their bulk material counterparts [20, 21]. This field is rapidly expanding with new entrants from different materials such as topological insulators [22, 23], hexa boronitride [24, 25], layered transition metal chalcogenides [26, 27] and metal oxides [28] for all of which single crystalline films are required but where still technological issues hinder the fabrication of well-controlled epitaxial films by commonly applied growth methods.

The preparation of these novel materials as ultra-thin layers is successfully addressed by the method of exfoliation. Eventhough exfoliation of thin and ultra-thin layers from bulk single crystals is not transferable to industrial processing it allows the fabrication of thin layers for research. Advantageously, the single crystalline films are prepared from a source material, namely the bulk crystals, which are well characterized in their material properties. In this work, we report on the successful exfoliation of β-Ga$_2$O$_3$ flakes in the ultra-thin (>2 nm) to thin (up to 300 nm) film regime. This is possible due to the monoclinic crystal structure.

In these single crystalline thin flakes minimal crystal and doping defects can be guaranteed due to the high quality of the source bulk single crystal. We proof that after the exfoliation and the micro device processing (photo lithography, metallization, lift off) these high-quality single crystalline flakes maintain the temperature-dependent bulk crystal properties in the intermediate thickness regime between 125 and 300 nm. This opens the route to the fabrication of ultra-thin layers of β-Ga$_2$O$_3$ flakes and the investigation of low-dimensional transport properties in this material.

2 Exfoliation, micro-contacts and structural characterization In order to systematically study the transport properties of thin β-Ga$_2$O$_3$ samples and compare them with those of bulk β-Ga$_2$O$_3$ samples measured in the past, we perform measurements in different tens of nanometer thick samples of several micrometer square area. The samples presented in this paper were obtained from a β-Ga$_2$O$_3$ single crystal grown from the melt by the Czochralski method [29]. The crystals show n-type conductivity and carrier densities ranging from $\sim 6 \times 10^{16}$ cm^{-3} to $\sim 8 \times 10^{17}$ cm^{-3} determined by Hall measurements [17].

Fig. 1a shows a photograph of an as-cleaved sample from the bulk β-Ga$_2$O$_3$ crystal, used for thin micro flakes preparation. Their electrical properties have been reported previously [17]. Micrometer-sized and few nanometer thick β-Ga$_2$O$_3$ flakes were prepared using a mechanical exfoliation technique with scotch tape. The (100) plane is the easy cleavage plane of the crystal. The exfoliation procedure was carried out on top of a 300 nm thick SiO$_2$ layer grown on a boron-doped Si substrate. The preparation of the micro flakes involved the following steps: Before sample preparation, the substrates were cleaned with acetone and then isopropanol in an ultrasonic bath for ~ 5 min. After sonication, drops of isopropanol were placed on the substrates and subsequently blow-dried with nitrogen. A $5 \times 2 \times 1$ mm^3 piece of the initial Ga$_2$O$_3$ crystal was glued
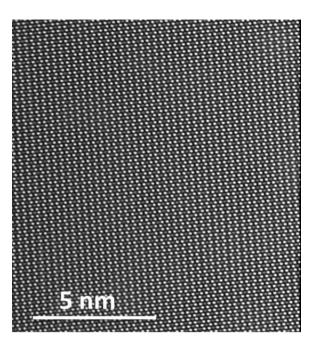

Figure 1 (a) Image of an as-cleaved β-Ga$_2$O$_3$ sample from a bulk crystal used for the flakes preparation. (b and c) Optical microscope images of two β-Ga$_2$O$_3$-flakes on SiO$_2$ (300 nm)/Si substrate prepared as described in the text. The thickness of these samples is: 120 and 60 nm, respectively. (d) Confocal microscopy image of a homogeneous 228 nm thick β-Ga$_2$O$_3$-sample. (e) Scanning electron microscope image of a β-Ga$_2$O$_3$-sample showing the layered structure at the edges. (f) AFM image of a 80 nm thin β-Ga$_2$O$_3$-sample.

Original

Paper

Phys. Status Solidi A 211, No. 3 (2014)
545

on a separate Si substrate using a GE7031 varnish. Using scotch tape, a thin layer of β-Ga$_2$O$_3$ was cleaved and then folded and unfolded back several times into the scotch tape, resulting in a subsequent cleaving of the layer into thinner and thinner flakes. The SiO$_2$/Si substrate was then placed on top of the sticky tape in a region uniformly covered by β-Ga$_2$O$_3$ flakes. By pressing gently on top of the substrate with a suitable tip, the β-Ga$_2$O$_3$ flakes were placed on the SiO$_2$ surface of the Si wafer due to the adhesive force. Immediately after the exfoliation process we put the substrate containing the β-Ga$_2$O$_3$ flakes in an ultrasonic bath during 15–30 s using highly concentrated acetone. This process cleans and helps to select only the well adhered β-Ga$_2$O$_3$ flakes on the substrate.

After the exfoliation process we used optical microscopy to select and mark the position of the flakes. Figures 1b and c show two of the investigated samples of different micrometer length and tens of nanometer thickness. The flakes are examined using a combination of confocal microscopy, atomic force microscopy (AFM), scanning electron microscopy (SEM) and transmission electron microscopy (TEM). Confocal microscopy is used to characterize thickness homogeneity and Fig. 1d shows the confocal microscope image of a 228 nm thick homogeneous β-Ga$_2$O$_3$-flake. Figure 1e shows the SEM image of β-Ga$_2$O$_3$-flake showing the layered structure at the edges. Figure 1f shows the AFM image of a 80 nm thick homogeneous β-Ga$_2$O$_3$-flake with a height profile.

Structural analysis using high-resolution TEM (HRTEM) was carried out at an aberration corrected FEI Titan 80–300 microscope operating at 300 kV. The samples for HRTEM characterization were prepared by cleaving the crystal in the (100) plane. The investigated samples were not subjected to any chemical or mechanical treatment or ion milling. One could simply cleave the samples of several atomic layers only by exploiting the easy cleavage planes. Thus, the as-cleaved samples are not externally damaged and could provide a picture of the real structure of the as-grown crystal. Figure 2 shows a typical high resolution image of 100×100 nm^2 area using negative spherical aberration and positive defocus conditions which results in bright atom contrast. From the exit wave reconstruction we can estimate the sample thickness, which is about 2.4 nm in the displayed region. The crystal is perfect and no extended defects are visible. The HRTEM image of the same crystal in the (201) plane can be seen in [29].
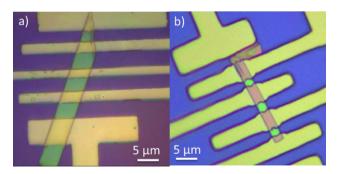
For the preparation of Ti/Au-electrical contacts on the β-Ga$_2$O$_3$-flakes we used micro-laser lithography. Positive photoresist AZECI 3027 was coated, and the samples were spun in open air for 40 s at speeds varying from 5200 to 5400 rpm. The thickness of the liquid layers became in the order of 350–400 nm. In the next steps micro-laser lithography was made to define the electrodes. We used oxygen and hydrogen plasma to remove the residual photoresist on the samples. By sputtering 70 nm Ti (99.99%) was deposited as contact material and 30–50-nm Au as cap layer under high vacuum conditions (basic

Figure 2 High resolution TEM image of Czochralski grown as-cleaved β-Ga$_2$O$_3$-sample of thickness 2.4 nm showing a defect-free structure. Plane orientation is (101). Bright spots correspond to Ga columns and spots with reduced intensity to oxygen columns. Spacing between atoms (bright spots) is about 1.5 Å.

pressure $< 10^{-5}$ mbar, argon pressure of 10^{-2} mbar). Lift-off processing completed the electrode fabrication and then the sample was glued on a chip carrier and carefully bonded. Figures 3a and b show two β-Ga$_2$O$_3$-flakes with lithographically patterned Ti/Au-contacts. Although the contact resistance may often be decreased by alloying, we did not apply such thermal treatment. This was done in order to prevent any side effects by diffusion processes in the electrical material characterization as the electrical contacts are only a few micrometer apart due to the small extension of the micro flakes.

3 Transport measurements Low-noise resistance measurements were performed by means of a conventional DC technique (Keithley 2401 sourcemeter and nano-voltmeter). Using a cryostat with 0.1 K temperature stability,

Figure 3 Optical microscope images of exfoliated β-Ga$_2$O$_3$-flakes with micro-patterned titanium-electrodes. The thickness of the flakes is: (a) 137 nm and (b) 65 nm.
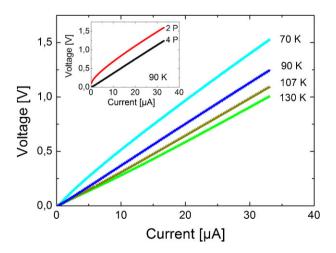
temperature-dependent resistance measurements were carried out for temperatures ranging from 30 K to room temperature. By transport measurements we investigated flakes of several micrometers in the lateral extensions. This size selection was required in order to fabricate contacts by micro-laser lithography. Therefore, our transport investigations cover the thickness range from 125 to 190 nm of the β-Ga$_2$O$_3$-flakes on which micrometer-sized contacts of Ti/Au- or Ti-electrodes were successfully fabricated.
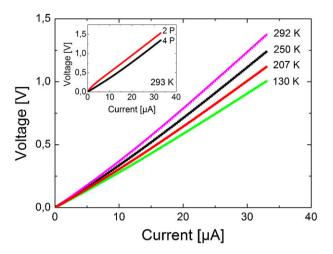
In four-point measurements the obtained $V(I)$ curves show linear characteristics up to 20 μA and from the slope the ohmic resistance was determined. We measured temperature-dependent four-probe $V(I)$ characteristics as shown exemplarily in Figs. 4 and 5 for a flake of 190 nm thickness. Selected $V(I)$-curves measured for temperatures between 70 and 130 K are plotted in Fig. 4 and show an increase of the resistance (slope) with decreasing temperature. Selected $V(I)$ characteristics measured from 130 K up to room temperature are depicted in Fig. 5. In this temperature range, the resistance is increasing for increasing temperature. The corresponding temperature-dependent resistivity in the full temperature range is depicted in Fig. 6.

The resistivity has a minimum near 130 K of $\rho \sim 1\,\Omega$ cm. For higher temperatures the resistivity increases up to about $\rho = 1.7\,\Omega$ cm at nearly 300 K. For lower temperature the resistivity is strongly enhanced beyond $\rho > 2\,\Omega$ cm below 50 K indicating a freeze-out of charge carriers. The influence of Joule heating by applied higher currents ($>20\,\mu$A) is clearly seen in Figs. 4 and 5. In the low-temperature regime, Fig. 4, Joule heating at higher currents lowers the resistance, while in the high-temperature regime, Fig. 5, it raises the resistance.

A comparison of typical four- and two-point measurements is shown in the insets of Fig. 4 for $T = 90$ K and Fig. 5 for $T = 293$ K. For currents above 20 μA the two-probe
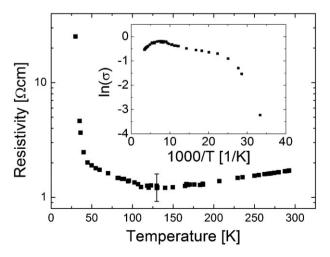

Figure 5 Voltage-current characteristics for a β-Ga$_2$O$_3$ 190 nm thin flake measured in four-point geometry at temperatures from 130 K up to 300 K: The resistance increases with increasing temperature. Inset: Comparison of two- and four-point measurements at 300 K. At currents above 20 μA the determined resistances are identical.

characteristic approaches the same resistances as obtained by the four-probe measurement, see insets in Figs. 4 and 5. However, in the two-point measurements, additionally, the influence of the contact resistance becomes apparent in the low-current regime and, hence, can be extracted. The temperature behaviour of the Ti/β-Ga$_2$O$_3$-contact resistance will be discussed further below.

The Arrhenius plot of the conductivity of the 190 nm thick β-Ga$_2$O$_3$ flake is shown in the inset of Fig. 6. For the temperatures ranging from 50 to 300 K, the V-I characteristics (see Figs. 4 and 5) are used to determine the conductivity of the β-Ga$_2$O$_3$ thin film. The equation

Figure 4 Voltage–current characteristics for a β-Ga$_2$O$_3$ 190 nm thin flake measured in four-point geometry from 70 K up to 130 K: The resistance decreases with increasing temperature. Inset: Comparison of two- and four-point measurements at 90 K. At currents above 20 μA the determined resistances are identical.

Figure 6 Temperature dependence of the resistivity. Inset: Arrhenius plot for the temperature dependence of conductivity. The activation energy obtained from the slope near room temperature is about -10.5 ± 0.4 meV.

Phys. Status Solidi A 211, No. 3 (2014)

547

$$\sigma = \sigma_0 \exp\{(-E_a/k_B T)\} \tag{1}$$
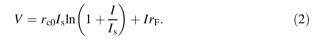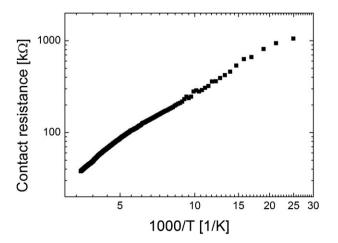
gives an activation energy of $E_a = (3.1 \pm 0.2)$ meV for $T < 100$ K and of $E_a = (-10.5 \pm 0.4)$ meV for $T > 150$ K. These results confirm the findings for the corresponding bulk β-Ga$_2$O$_3$ single crystals [17]. The temperature dependence of the bulk mobility shows a maximum near 100 K [17]. This corresponds well with the minimum in resistivity as observed for the β-Ga$_2$O$_3$ flake. However, the absolute value of the resistivity depends on the doping level. At room temperature, we estimate a value of $n \leq 5 \times 10^{16}$ cm^{-3} making use of the mobility of 130 cm^2 V^{-1} s^{-1} as determined for the corresponding bulk crystal [17].

In the following we discuss the determination of the total contact resistance for the Ti/β-Ga$_2$O$_3$ contacts, its temperature dependence and ageing phenomena.
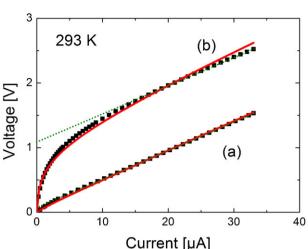
In Fig. 7, the temperature dependence of the contact resistance r_c is plotted. We find a linear increase of r_c with increasing inverse temperature. The contact resistance was determined from the slope of the two-point $V(I)$ characteristic as discussed below with $r_{c0} = r(I=0) - r_F$. Here, $r(I=0)$ follows from the slope of $V(I)$ at I near zero and r_F from the slope at $V(I = 20 \, \mu\text{A})$.

The two-point $V(I)$ characteristics are dominated by the series of resistances of the β-Ga$_2$O$_3$-flake denoted by r_F and the two metal–semiconductor contacts with the contact resistance r_c, examples are given in Fig. 8. Here, I is the driving current and V is the measured voltage. We approximate the $I(V)$ function [30] as $I = I_s \exp[(V - Ir_F)/2V_T]$, where $V_T = k_B T/e$ is the thermal voltage, also depicted as threshold voltage, see further below. k_B depicts the Boltzmann constant, e the elementary charge. $I_s = 2V_T/r_{c0}$ where r_{c0} is the total contact resistance of the two Ti/β-Ga$_2$O$_3$ contacts at zero driving current. The $V(I)$-characteristics is then given by

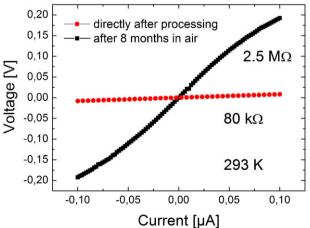$$V = r_{c0} I_s \ln\left(1 + \frac{I}{I_s}\right) + Ir_F. \tag{2}$$

Figure 8 $V(I)$ characteristics (filled square symbols) measured in two-point geometry at $T = 293$ K for two different contacts: (a) Au-capped Ti electrodes on β-Ga$_2$O$_3$ and (b) uncapped Ti electrodes on β-Ga$_2$O$_3$ after 8 months in air. At high currents ($I > 20 \, \mu$A) the slope yields an approximate value for the material resistance and from the slope at zero current the contact resistance is determined. Fits to the measurements were made according to Eq. (2) (solid red lines). A comparison of the four- and two-point measurements of the Au-capped Ti-β-Ga$_2$O$_3$ flake in (a) at $T = 293$ K is plotted in the inset of Fig. 5.

From this a total differential resistance $r(I)$ follows

$$r = \frac{r_{c0}}{1 + I/I_s} + r_F. \tag{3}$$

The Ti/β-Ga$_2$O$_3$ contact resistance at zero current r_{c0} and the resistance of the β-Ga$_2$O$_3$ flake r_F are determined experimentally from the slope of the $V(I)$ curves according to Eq. (2) at low and high currents, respectively. The linear approximation of the $V(I)$ curve at high currents gives

Figure 7 Temperature dependence of the Ti-β-Ga$_2$O$_3$ total contact resistance (r_c).

Figure 9 Voltage–current characteristic of a β-Ga$_2$O$_3$-flake with Ti electrodes without Au cap layer: measured immediately after contacting with titanium (red circles) and 8 months later after storage in air (black squares).

$$V = r_{c0}I_s + r_F I = 2V_T + r_F I. \qquad (4)$$

Here, r_F is determined by the slope and the extrapolation to zero current delivers $2V_T$.

From $V(I)$-characteristics as measured for a β-Ga$_2$O$_3$-flake with Ti/Au electrodes, labelled (a) in Fig. 8, we determine $2V_T = 55$ mV and hence, $V_T = 27.5$ mV. This value corresponds well to $V_T = 25$ mV at room temperature. The slight increase of $+2.5$ mV above the expected room temperature value may find its explanation in Joule heating at higher currents as discussed before (see Figs. 3 and 4).

For Ti electrodes without Au capping, the above reported contact resistance is determined directly after the device processing. However, for Ti electrodes without an Au cap layer considerable ageing is observed if the sample is stored in air, as is depicted by the $V(I)$ curve in Fig. 9. In such a case, we determine a much higher value of $V_T = 550 \pm 3$ mV which strongly exceeds $k_B T/e$. However, it corresponds well to a value given by a donor-like trap level $E_T = 0.55$ eV as determined from bulk β-Ga$_2$O$_3$ single crystals by DLTS measurements [17]. If such a trap level occurs, the V_T denotes a threshold voltage and is given by the expression $V_T = k_B T/e + E_T$. Here, the thermal contribution of $k_B T/e$ is two orders of magnitude smaller and therefore hidden by the experimental error. We explain the origin of the donor-like trap levels by ageing of the uncapped Ti-contacts due to the exposure to air oxygen.

4 Discussion and outlook As shown by this study, the method of exfoliation can be reliably applied to produce β-Ga$_2$O$_3$ flakes in the ultra-thin (>2 nm) to thin (up to 300 nm) thickness regime. This is possible due to the monoclinic crystal structure and opens a route to investigate the material properties of β-Ga$_2$O$_3$ as thin and ultra-thin films. In such high-quality single crystalline layers a lower bound in the density of crystal and doping defects can be realized. Therefore exfoliated single crystalline β-Ga$_2$O$_3$-films may serve as reference material: It will be of interest whether this film quality can be approached by epitaxial growth methods in the future.

Furthermore, we demonstrated that the single crystalline bulk electrical material properties are maintained in β-Ga$_2$O$_3$ flakes above 100 nm thickness. The determined activation energies correspond well to that of bulk β-Ga$_2$O$_3$ single crystals [17]. From the bulk mobility, we estimate that a value of $n(300\,\mathrm{K}) < 5 \times 10^{16}$ cm^{-3} delivers an upper limit and confirms the value of the bulk crystal of highest purity. This means that the process of exfoliation and microdevice processing does not affect the high-crystal quality of the source bulk material. Because we used high-purity single-crystalline flakes the observed temperature-dependent electrical properties are not influenced by grain boundaries as in polycrystalline thin films. In this work, we were restricted to the thin film regime by the micrometer-sized electrical contacts. By nanolithography micron-size β-Ga$_2$O$_3$ flakes in the ultra-thin film regime can be contacted. This will allow the investigation of transport phenomena in the cross-over regime from three- to quasi-two-dimensional layers. Such thickness-dependent investigation will give insight to the surface contributions in transport.

In order to attain high-performance and long-life operation in optical and electrical devices using β-Ga$_2$O$_3$ thin films it is essential to achieve metal-semiconductor contacts that have a low resistance, are thermally stable and reliable [15]. The major loss of device performance is mostly caused by a high resistance metal/semiconductor interface through contact failures having potential barriers and/or thermal stress. Here, we showed that the preparation of Ti/Au-electrical contacts to exfoliated β-Ga$_2$O$_3$ thin films is feasible. This is notable as the contact preparation differs strongly from that usually applied to bulk crystals (formation of contacts by a capacitive discharge sintering process). We expect that a further decrease of the contact resistance may be achieved by alloying. However, in order to exclude any influence of a thermal treatment on the β-Ga$_2$O$_3$ material properties in micro- and nanodevices a study of diffusion of the contact metal (Ti) in β-Ga$_2$O$_3$ thin films is required. With respect to longterm operation, ageing of the Ti contacts to a β-Ga$_2$O$_3$ thin film microdevice may be prevented by a cap layer of Au. This is crucial, otherwise the threshold voltage for driving a current through the contact may strongly increase due to donor-like trap levels due to the exposure of Ti to air oxygen.

With regard to the temperature dependence we find that the contact resistance for a non-alloyed Ti-β-Ga$_2$O$_3$ contact grows inversely with temperature as expected for thermionic emission. At room temperature the choice of the regime of the current density for operation determines whether the contact resistance plays an important role. For β-Ga$_2$O$_3$ microflakes in the thickness range of about 100 nm the Ti/β-Ga$_2$O$_3$ contact resistance becomes comparable to the resistance of microflake for low-current densities of $j < 100$ A cm^{-2}. However, for high-current densities $j > 100$ A cm^{-2} this contact resistance appears negligible. For high-power devices, it is of interest to estimate the power density applied to the β-Ga$_2$O$_3$ thin films investigated. In the regime of low-current densities $j < 100$ A cm^{-2} ($I \sim 3$ μA) we estimate a power density of 10^4 W cm^{-3}. Instead, in the regime of high-current densities $j > 100$ A cm^{-2} ($I \sim 30$ μA) high-power densities of nearly 1 MW cm^{-3} are approached. In this high-power regime the material properties of β-Ga$_2$O$_3$ dominate the electrical measurements of the microflakes.

5 Conclusions By exfoliation β-Ga$_2$O$_3$ micro flakes can be prepared in the range of 2 nm to a few hundred nanometer thickness. Transmission electron microscopy of exfoliated β-Ga$_2$O$_3$ ultra-thin films shows a defect-free structure. In exfoliated nearly-defect free single crystalline layers above 100 nm thickness the bulk material properties are preserved despite exfoliation and micro device processing techniques. Therefore, such films may serve as reference materials for investigations of thickness-dependent transport

phenomena in exfoliated or epitaxially grown ultra-thin β-Ga$_2$O$_3$ layers. The exfoliated single crystalline films possess electrical properties which compare to those of the source bulk single crystals with the highest purity and mobility. We find that at high-current densities $j > 100\,\mathrm{A\,cm^{-2}}$ and with increasing temperature the Ti-β-Ga$_2$O$_3$ metal-semiconductor contact resistance can be neglected compared to the thin film resistance. In this regime of high-power densities the material properties of the β-Ga$_2$O$_3$ microflakes dominate the electrical transport which is important for high power applications.

References

[1] H. H. Tippins, Phys. Rev. **140**, A316 (1965).

[2] M. Orita, H. Ohta, M. Hirano, and H. Hosono, Appl. Phys. Lett. **77**, 4166 (2000).

[3] M. Grundmann, H. Frenzel, A. Lajn, M. Lorenz, F. Schein, and H. v. Wenckstern, Phys. Status Solidi A **207**, 1437–1449 (2010).

[4] M. Higashiwaki, K. Sasaki, A. Kuramata, T. Masui, and S. Yamakoshi, Appl. Phys. Lett. **100**, 013504 (2012).

[5] M. Orita, H. Hiramatsu, H. Ohta, M. Hirano, and H. Hosono, Thin Solid Films **411**, 134 (2002).

[6] T. Miyata, T. Nakatani, and T. Minami, J. Lumin. **87–89**, 1183–1185 (2000).

[7] K. Matsuzaki, H. Hiramatsu, K. Nomura, H. Yanagi, T. Kamiya, M. Hirano, and H. Hosono, Thin Solid Films **496**, 37 (2006).

[8] M. Ogita, K. Higo, Y. Nakanishi, and Y. Hatanaka, Appl. Surf. Sci. **175–176**, 721, (2001).

[9] K. Matsuzaki, H. Yanagi, T. Kamiya, H. Hiramatsu, K. Nomura, M. Hirano, and H. Hosono, Appl. Phys. Lett. **88**, 092106 (2006).

[10] Z. Li, B. Zhao, P. liu, and Y. Zhang, Microelectron. Eng. **85**, 1618–1620 (2008).

[11] L. Dai, X. L. Chen, X. N. Zhang, A. Z. Jin, T. Zhou, B. Q. Hu, and Z. Zhang, J. Appl. Phys. **92**, 1062 (2002).

[12] S.-L. Ou, D.-S. Wuu, Y.-C. Fu, S.-P. Liu, R.-H. Horng, L. Liu, and Z.-C. Feng, Mater. Chem. Phys. **133**, 700705 (2012).

[13] M.-Y. Tsai, O. Bierwagen, M. E. White, and J. S. Speck, J. Vac. Sci. Technol. A **28**, 354 (2010).

[14] Y. Zhang, J. Yan, Q. Li, C. Qu, L. Zhang, and W. Xie, Mater. Sci. Eng. B **176**, 846849 (2011).

[15] P. D. C. King and T. D. Veal, J. Phys.: Condens. Matter. **23**, 334214 (2011).

[16] M. R. Lorenz, J. F. Woods, and R. J. Gambino, J. Phys. Chem. Solids **28**, 403–404 (1967).

[17] K. Irmscher, Z. Galazka, M. Pietsch, R. Uecker, and R. Fornari, J. Appl. Phys. **110**, 063720 (2011).

[18] Y. Jeliazova and R. Franchy, Surf. Sci. **527**, 57–70 (2003).

[19] H. Kim and W. Kim, J. Appl. Phys. **62**, 2000 (1987).

[20] A. K. Geim and I. V. Grigorieva, Nature **499**, 423 (2013).

[21] M. Xu, T. Liang, M. Shi, and H. Chen, Chem. Rev. **113**, 37663798 (2013).

[22] Md Z. Hossain, S. L. Rumyantsev, K. M. F. Shahil, D. Teweldebrhan, M. Shur, and A. A. Balandin, ACS Nano **5**, 2657 (2011).

[23] D. Teweldebrhan, V. Goyal, and A. A. Balandin, Nano Lett. **10**, 12091218 (2010).

[24] G.-H. Lee, Y.-J. Yu, C. Lee, C. Dean, K. L. Shepard, P. Kim, and J. Hone, Appl. Phys. Lett. **99**, 243114 (2011).

[25] C. R. Dean, A. F. Young, I. Meric, C. Lee, L. Wang, S. Sorgenfrei, K. Watanabe, T. Taniguchi, P. Kim, K. L. Shepard, and J. Hone, Nature Nanotechnol. **5**, 722 (2010).

[26] J. Khan, C. M. Nolen, D. Teweldebrhan, D. Wickramaratne, R. K. Lake, and A. A. Balandin, Appl. Phys. Lett. **100**, 043109 (2012).

[27] P. Goli, J. Khan, D. Wickramaratne, R. K. Lake, and A. A. Balandin, Nano Lett. **12**, 5941–5945 (2012).

[28] Y. Wang, C. Sun, J. Zou, L. Wang, S. Smith, G. Q. Lu, and D. J. H. Cockayne, Phys. Rev. B. **81**, 081401(R) (2010).

[29] Z. Galazka, R. Uecker, K. Irmscher, M. Albrecht, D. Klimm, M. Pietsch, M. Brützam, R. Bertram, S. Ganschow, and R. Fornari, Cryst. Res. Technol. **45**, 1229 (2010).

[30] S. M. Sze and K. K. Ng, in: Physics of Semiconductor Devices, 3rd ed. (John-Wiley & Sons, Hoboken, 2007), chap. 3.